THE JOURNAL OF BIOLOGICAL CHEMISTRY
Vol. 278, No. 37, Issue of September 12, pp. 34990–34997, 2003
Printed in U.S.A.

Molecular Identification of a Functional Homologue of the Mammalian Fatty Acid Amide Hydrolase *in Arabidopsis thaliana**

Received for publication, May 28, 2003, and in revised form, June 20, 2003
Published, JBC Papers in Press, June 24, 2003, DOI 10.1074/jbc.M305613200

Rhidaya Shrestha‡, Richard A. Dixon§, and Kent D. Chapman‡¶

From the ‡Department of Biological Sciences, Division of Biochemistry and Molecular Biology, University of North Texas, Denton, Texas 76203 and §Plant Biology Division, Samuel Roberts Noble Foundation, Ardmore, Oklahoma 73401

***N*-Acylethanolamines (NAEs) are endogenous constituents of plant and animal tissues, and in vertebrates their hydrolysis terminates their participation as lipid mediators in the endocannabinoid signaling system. The membrane-bound enzyme responsible for NAE hydrolysis in mammals has been identified at the molecular level (designated fatty acid amide hydrolase, FAAH), and although an analogous enzyme activity was identified in microsomes of cotton seedlings, no molecular information is available for this enzyme in plants. Here we report the identification, the heterologous expression (in *Escherichia coli*), and the biochemical characterization of an *Arabidopsis thaliana* FAAH homologue. Candidate *Arabidopsis* DNA sequences containing a characteristic amidase signature sequence (PS00571) were identified in plant genome data bases, and a cDNA was isolated by reverse transcriptase-PCR using *Arabidopsis* genome sequences to develop appropriate oligonucleotide primers. The cDNA was sequenced and predicted to encode a protein of 607 amino acids with 37% identity to rat FAAH within the amidase signature domain (18% over the entire length). Residues determined to be important for FAAH catalysis were conserved between the *Arabidopsis* and rat protein sequences. In addition, a single transmembrane domain near the N terminus was predicted in the *Arabidopsis* protein sequence, similar to that of the rat FAAH protein. The putative plant FAAH cDNA was expressed as an epitope/His-tagged fusion protein in *E. coli* and solubilized from cell lysates in the nonionic detergent, dodecyl maltoside. Affinity-purified recombinant protein was indeed active in hydrolyzing a variety of naturally occurring *N*-acylethanolamine types. Kinetic parameters and inhibition data for the recombinant *Arabidopsis* protein were consistent with these properties of the enzyme activity characterized previously in plant and animal systems. Collectively these data now provide support at the molecular level for a conserved mechanism between plants and animals for the metabolism of NAEs.**

N-Acylethanolamines (NAEs)[1] are lipid mediators that are produced from the phospholipase D-mediated hydrolysis of *N*-acylphosphatidylethanolamines, a minor membrane lipid constituent of cellular membranes (1). In animal systems, anandamide (NAE 20:4) acts as an endogenous ligand for cannabinoid receptors and has varied physiological roles, such as the modulation of neurotransmission in the central nervous system (2). Anandamide also activates vanilloid receptors, functions as an endogenous analgesic (3), and appears to be involved in neuroprotection (4, 5). In other tissues, NAEs have been implicated in immunomodulation (6), synchronization of embryo development (7), and induction of apoptosis (8). These endogenous bioactive molecules lose their signaling activity upon hydrolysis by fatty acid amide hydrolase (FAAH; see Ref. 9).

In plants NAEs are present in substantial amounts in desiccated seeds (~1 $\mu g\ g^{-1}$ fresh weight), and their levels decline after a few hours of imbibition (10). Individual NAEs were identified predominantly as 12C, 16C, and 18C species with *N*-linoleoylethanolamine (NAE 18:2) generally being the most abundant. Like in animal cells, NAEs are derived from *N*-acylphosphatidylethanolamines (11, 12) by the action of a phospholipase D (13, 14). The occurrence of NAEs in seeds and their rapid depletion during seed imbibition to barely detectable levels in seedlings (12) suggests that these lipids may have a role in the regulation of seed germination and normal seedling development. In fact, recent experiments with *Arabidopsis thaliana* seedlings showed that when seeds were germinated and maintained on elevated levels (micromolar concentrations) of the naturally occurring NAE 12:0, seedling roots developed abnormally in a manner consistent with a disruption of both normal cell division and cellular expansion (15), signifying the importance of regulating NAE levels for normal plant growth and development.

The concept of NAEs acting as lipid mediators in plant systems is supported by an increasing amount of experimental evidence in vegetative tissues where normal levels of NAEs are quite low (low nanomolar concentrations). For example, NAE 14:0 appears to function as an endogenous modulator of pathogen elicitor signaling by plant cells (12, 16). NAE 14:0 levels, quantified by gas-liquid chromatography-mass spectrometry, increased 10–50-fold in leaves of tobacco plants that were treated for a few minutes with either xylanase or cryptogein elicitor proteins (17). These "elicitor-activated" levels of NAE 14:0 (submicromolar concentrations) were sufficient to induce defense gene expression (*e.g.* phenylalanine ammonia-lyase and PAL2 transcript abundance) in tobacco plants within hours of treatment in a manner similar to but independent of

* This work was supported by Grant 2002-35318-12571 from the United States Department of Agriculture-National Research Initiative Competitive Grants Program. The costs of publication of this article were defrayed in part by the payment of page charges. This article must therefore be hereby marked "*advertisement*" in accordance with 18 U.S.C. Section 1734 solely to indicate this fact.

The nucleotide sequence(s) reported in this paper has been submitted to the GenBank™/EBI Data Bank with accession number(s) AY308736.

¶ To whom correspondence should be addressed. Tel.: 940-565-2969; Fax: 940-565-4136; E-mail: chapman@unt.edu.

[1] The abbreviations used are: NAE, *N*-acylethanolamine; AS, amidase signature; BisTris, 2-[bis(2-hydroxyethyl)amino]-2-(hydroxymethyl)propane-1,3-diol; CHAPS, 3-[(3-cholamidopropyl)dimethylammonio]-1-propanesulfonic acid; DDM, *n*-dodecyl β-D-maltoside; FAAH, fatty acid amide hydrolase; FFA, free fatty acid; IPTG, isopropyl-β-D-thiogalactopyranoside; MAFP, methyl arachidonyl fluorophosphonate; NAE 12:0, *N*-lauroylethanolamine; NAE 14:0, *N*-myristoylethanolamine; NAE 16:0, *N*-palmitoylethanolamine; NAE 18:2, *N*-linoleoylethanolamine; NAE 20:4, *N*-arachidonoylethanolamine (anandamide); PMSF, phenylmethylsulfonyl fluoride; RT, reverse transcriptase; WT, wild type; UTR, untranslated region; TIGR, Institute for Genomic Research.

elicitor proteins (17). Mammalian cannabinoid receptor antagonists at concentrations equimolar to NAE blocked the activation of defense gene expression induced by either NAEs or by fungal elicitor proteins (16). A membrane-associated protein was identified in leaves of tobacco (and other plant species), which specifically bound to [^{3}H]NAE 14:0 with high affinity (K_d in the low nanomolar range). This NAE 14:0-binding protein was proposed to mediate the NAE activation of PAL2 expression in tobacco leaves, a conclusion that was based on the similarities between NAE binding properties *in vitro* and NAE-induced physiological responses *in vivo*, including experiments with cannabinoid receptor antagonists (16). Although some clear differences are evident between the emerging NAE signaling pathway in plants and the better characterized endocannabinoid signal pathway of animals, there appear to be some remarkable similarities in the formation and perception of bioactive acylethanolamides by these two diverse groups of multicellular organisms. Likewise, we propose that an FAAH-like mechanism operates in plants for NAE signal termination and overall regulation of NAE levels under various physiological conditions.

Recently, depletion of NAEs during seed imbibition/germination was determined to occur via two metabolic pathways: one lipoxygenase-mediated for the formation of NAE oxylipins from NAE 18:2, and one amidase-mediated for hydrolysis of saturated and unsaturated NAEs (18). Hydrolysis of NAEs was reconstituted and characterized in microsomes of cottonseeds and appeared to be catalyzed by an enzyme similar to the FAAH of mammalian species (18). Here we report the identification of a plant orthologue of mammalian FAAH by bioinformatic approaches, isolation of its cDNA sequence, expression of this cDNA in *Escherichia coli*, and identification of the protein product as an NAE amidohydrolase. These results support our previous studies on the metabolism of NAEs in plant tissues and for the first time provide molecular evidence for a conserved pathway in both plants and animals for the hydrolysis of NAEs. Moreover, the results of this research now provide a means to manipulate the levels of endogenous NAEs in plants to evaluate the physiological role(s) of these bioactive lipids.

EXPERIMENTAL PROCEDURES

Materials—[1-^{14}C]Arachidonic acid was purchased from PerkinElmer Life Sciences, and [1-^{14}C]lauric acid was from Amersham Biosciences. [1-^{14}C]Myristic acid, arachidonic acid, lauric acid, linoleic acid, myristic acid, anandamide, ethanolamine, phenylmethylsulfonyl fluoride (PMSF), and isopropyl-β-D-thiogalactopyranoside (IPTG) were from Sigma. [1-^{14}C]Linoleic, [1-^{14}C]palmitic acids, and [1,2-^{14}C]ethanolamine were purchased from PerkinElmer Life Sciences. Ceramide was from Avanti Polar Lipids (Alabaster, AL), and 2-arachidonyl glycerol was from Cayman Chemical (Ann Arbor, MI). Methyl arachidonyl fluorophosphonate (MAFP) was from Tocris Cookson, Inc. (Ellisville, MO); *n*-dodecyl β-D-maltoside (DDM) was from Calbiochem, and Silica Gel G (60 Å)-coated glass plates for thin layer chromatography (20 × 20 cm, 0.25 mm thickness) were from Whatman. Specific types of *N*-[1-^{14}C]acylethanolamines (and non-radiolabeled NAEs) were synthesized from ethanolamine and the respective 1-^{14}C-labeled fatty acids (and non-radiolabeled FFAs) by first producing the fatty acid chloride (19) and purified by TLC as described elsewhere (18).

Bioinformatics and cDNA Isolation—BLAST searches (blast.wustl.edu) in various data bases were done using the amidase signature (AS) consensus block embedded in rat FAAH (blocks.fhcrc.org). DNA sequences containing a characteristic AS sequence (PS00571) were identified in the *A. thaliana* genome data base annotated by the Institute for Genomic Research (TIGR) and available at www.tigr.org, and one candidate *Arabidopsis* FAAH orthologue, At5g64440, was selected for further analyses. This selection was based largely on results from sequence analysis tools and data base comparisons including BLAST and cDART (www.ncbi.nlm.nih.gov), ProDom (20), Prosite (21), TMHMM transmembrane and topology predictor (22, 23), and pSORT (24). Sequence alignments and some sequence analyses were made with DNASIS software (Hitachi).

Sequence-specific primers were designed within the 5′- and 3′-UTR regions of At5g64440 based on predicted exon sequences and were used for reverse transcriptase (RT)-PCR (forward, 5′-CATTCAAGTTCCCAACAACTTCACCGC-3′ and reverse, 5′-GTCGACGTAAGAAATTCCAACACGG-3′). The template for RT-PCR was total RNA-extracted from the leaves of mature *Arabidopsis* plants using Trizol reagent (Invitrogen). Fresh leaf tissue (100 mg) was harvested, ground to a fine powder in liquid nitrogen, and combined with 2 ml of Trizol reagent for RNA isolation according to the manufacturer's instructions. For RT-PCR, the first strand cDNA synthesis from total RNA was carried out at 50 °C for 30 min and incubated for 4 min at 94 °C before the targeted amplification of the At5g64440 mRNA by Platinum *Taq* (RT-PCR mixture; Invitrogen) was achieved through 25 cycles of 94 °C for 1 min, 45 °C for 1 min, and 72 °C for 2 min followed by a final polymerization step at 72 °C for 7 min. The RT-PCR product was gel-purified and ligated into pTrcHis for nucleotide sequencing. Commercial DNA sequencing of both strands (complete 2× each strand) verified the identity of the cDNA as the AT5g64440 gene product, and the complete cDNA sequence was deposited in GenBank™.

Protein Expression—For protein expression, oligonucleotide primers (forward, 5′-ATGGGTAAGTATCAGGTCATGAAACG-3′ and reverse, 5′-GTTTGTATTGAGAATATCATAAAAGATTGC-3′) were designed to amplify only the open reading frame of the above At5g64440 cDNA, and PCR conditions were as above, except that a 10-to-1 ratio of polymerases (*Taq*-to-Pfu; Invitrogen) was used for amplification, and the template was the RT-PCR product (GenBank™ AY308736) in pTrcHis. The open reading frame-PCR product was gel-purified as above and subcloned into expression vectors, pTrcHis and pTrcHis2, and the constructs were introduced into chemically competent *E. coli* TOP10 cells as host. Transformed colonies were selected with correct in-frame fusions and cDNA sequence by sequencing of plasmid DNA over the vector insert junctions and by sequencing the inserts completely on both strands.

Selected transformed cell lines were grown in LB medium without glucose to an A_{600} of 0.6 to 0.7 and induced with 1 mM IPTG for 4 h. Pelleted cells were resuspended in lysis buffer (50 mM Tri-HCl, pH 8.0, 100 mM NaCl, and 0.2 mM DDM) at a ratio of 1-to-10^8 (*E. coli* cells-to-DDM molecules; assuming 0.1 A_{600} = 10^8 cells/ml, see Ref. 25). After incubation on ice for 30 min, resuspended cells were sonicated on ice with six 10-s bursts at high intensity with a 10-s cooling (ice bath) period between each burst. The selection of DDM as the detergent, and determination of optimal DDM concentration and content ratio was based on empirical comparisons for recovery of solubilized active enzyme with the highest specific activity. By the same criteria, DDM was determined to be better for solubilizing active enzyme than either Triton X-100 or CHAPS.

Solubilization and Ni^{2+} Affinity Purification—Routinely, cultured cells (50 ml) were pelleted, resuspended in 8 ml of native binding buffer (50 mM $NaPO_4$ buffer, pH 8.0, and 0.5 M NaCl) with 8 mg of lysozyme (Sigma) and 0.2 mM DDM (final), incubated on ice for 30 min, and disrupted by sonication as above. The crude lysate was centrifuged at 105,000 × *g* for 1 h in a Sorvall Discovery 90 model ultracentrifuge (Beckman Ti45 rotor). The supernatant was combined with ProBond resin, precharged with Ni^{2+}, and gently agitated for 60 min to keep the resin suspended in the lysate supernatant. The resin with adsorbed protein was settled, and the supernatant was aspirated off. The resin was washed 4 times to remove nonspecific proteins, and the adsorbed proteins were eluted with imidazole-containing buffer. Eluted proteins were concentrated, and imidazole was removed with 50 mM Tris-HCl, pH 8.0, 100 mM NaCl, and 0.2 mM DDM by filtration-centrifugation using Centricon YM-30 (Millipore, Bedford, MA) devices. Affinity-purified proteins were stored at −80 °C in 10% glycerol and were stable for more than 2 months.

Gel Electrophoresis and Western Blotting—Protein samples were diluted in 60 mM Tris-HCl, pH 6.8, 2% SDS, 10% glycerol, 0.025% bromphenol blue in 1:1 ratio and separated on 8 cm, precast 10% polyacrylamide/SDS gels (Bio-Rad) at 35 mA for 30 min and 60 mA for 60 min. For Western blot analysis, separated proteins were electrophoretically transferred to polyvinylidene fluoride (0.2 μm, Bio-Rad) membrane in a Semidry Trans-Blot apparatus (Bio-Rad) for 30 min at constant 14 V. Recombinant proteins expressed as c-Myc-epitope fusions were localized with 1-to-5000 dilution of anti-c-Myc antibodies (mouse monoclonal, Invitrogen) and detected by chemiluminescence (Bio-Rad substrate solutions) following incubation with 1-to-2500 dilution of goat anti-mouse IgG conjugated to horseradish peroxidase (Bio-Rad).

NAE Amidohydrolase Assays—NAE substrates were synthesized

and purified, and enzyme assays were conducted as described previously (18) with a few modifications. Generally the enzyme source was incubated with 100 μM [^{14}C]NAE (20,000 dpm) in 50 mM BisTris buffer, pH 9.0, for 30 min to survey for NAE amidohydrolase activity (18). Enzyme activity was examined for time, temperature, protein, and substrate concentration dependence. For enzyme characterization, reactions were initiated with 1 μg of affinity-purified protein and incubated at 30 °C with shaking for 30 min. Assays of lysates of *E. coli* cells expressing rat FAAH (WT-FAAH; Ref. 26) served as a comparison of NAE amidohydrolase activity, whereas non-transformed cell lysates or cell lysates with the *Arabidopsis* cDNA cloned in reverse orientation with respect to the *lacZ* promoter served as negative controls for activity assays. Enzyme assays were terminated by the addition of boiling isopropyl alcohol (70 °C), and lipids were extracted into chloroform. Lipid products were separated by TLC, and the distribution of radioactivity was evaluated by radiometric scanning (18). Activity was calculated based on the radiospecific activity of ^{14}C-labeled substrate. A general serine hydrolase inhibitor, phenylmethylsulfonyl fluoride (PMSF), and an irreversible active site-directed FAAH inhibitor, MAFP, were used to probe the sensitivity of recombinant *Arabidopsis* NAE amidohydrolase activity. Inhibitors were added from stock solutions dissolved in isopropyl alcohol for PMSF or Me_2SO for MAFP, and activity was adjusted for minimal solvent effects where necessary based on assays in the presence of the appropriate amount of solvent alone. Protein content was determined by Coomassie Blue dye binding using bovine serum albumin as the protein standard (27).

RESULTS

Tentative Identification of Arabidopsis NAE Amidohydrolase—In animal tissues, fatty acid amide hydrolase (EC 3.5.1.4), a member of the amidase signature (AS) family (28, 29), hydrolyzes NAEs to produce FFA and ethanolamine (30). A similar enzymatic activity was characterized previously in cottonseed microsomes (18). Mammalian FAAH enzymes have a conserved stretch of ~130 amino acids (31) containing a Ser/Ser/Lys catalytic triad (32). The predicted amidase structure has a central conserved motif of GGSS(G/A/S)G (33), and a somewhat longer stretch of amino acids G(GA)S(GS)(GS)G*X*(GSA)(GSAVY)*X*(LIVM)(GSA)*X*(6)(GSAT)*X*(GA)*X*(DE)*X*(GA)*X*S(LIVM)R*X*P(GSAC) is present in all enzymes of the amidase class (PS00457). Two serine residues at 217 and 241, highly conserved in the AS sequence, were found essential for enzymatic activity of recombinant rat FAAH (34). Mutation of either one of the residues into alanine caused complete loss of activity of the enzyme (34, 35). Also, mutation of serine 218 into alanine caused marked loss of activity (35). Taking these conserved residues in the AS consensus sequence into consideration, several putative plant orthologues were identified computationally. BLAST searches[2] in various data bases using the AS consensus block embedded in rat FAAH (blocks.fhcrc.org) identified one *A. thaliana* gene (*At5g64440*) that was selected for further characterization (Fig. 1).

The structure and organization of the *At5g64440* gene is relatively complex with 21 exons including 5′-UTR (untranslated region) and 3′-UTR (Fig. 1*A*). The predicted gene is 4689 nucleotides in length and encodes a predicted protein of 607 amino acids with a molecular mass of 66.1 kDa. Based on the presence of the conserved residues characteristic of the canonical AS sequence, this gene seemed likely to encode an *Arabidopsis* NAE amidohydrolase. To assess if this gene was expressed and to isolate a full-length cDNA for functional studies, oligonucleotide primers were designed within the 5′- and 3′-UTR, and a cDNA fragment was amplified by RT-PCR from *Arabidopsis* leaf RNA (Fig. 1*B*). The RT-PCR product was sequenced and found to be 99.9% identical with the corresponding TC139316 annotated at TIGR. The protein domain prediction tools, ProDom (20), identified six domain families in the *Arabidopsis* protein, five of which were also found in rat FAAH (Fig. 1*C*). A single putative transmembrane segment was identified near the N terminus (TMHMM; Refs. 22 and 23) similar to the predicted topological organization in rat FAAH.

Alignment of the deduced amino acid sequences from the *Arabidopsis* NAE amidohydrolase cDNA and the rat FAAH (28) showed only 18.5% identity over the entire length. Alignment within the AS sequence of 125 amino acids (Fig. 2*A*, *underlined residues*) showed 37% identity with five residues determined to be important for catalysis to be absolutely conserved (Ref. 31; Lys-142, Ser-217, Ser-218, Ser-241, and Arg-243, denoted by *arrows*; Fig. 2*A*). Comparison of a 47-amino acid motif within the AS showed the *Arabidopsis* protein had close to 60% identity with FAAHs from several mammalian species (Fig. 2*B*). Organization of predicted secondary structure within this *Arabidopsis* and rat FAAH AS motif was similar (Fig. 2*C*), and the structure of the rat enzyme has been confirmed by x-ray crystallography (36). In addition, this putative *A. thaliana* NAE amidohydrolase and rat FAAH have similar predicted molecular weights (~66 kDa), similar predicted topologies (single transmembrane segment near the N terminus with the C terminus facing the cytosol, via TMHMM transmembrane and topology predictor; Refs. 22 and 23), and similar predicted subcellular locations (secretory pathway, pSORT; Ref. 24). Although the *Arabidopsis* NAE amidohydrolase shared several domains with glutamyl-tRNA amidotransferases (Fig. 1*C*), these amino acid-modifying enzymes are localized to chloroplasts in higher plants, and there is no indication of stromal targeting sequences at the N terminus of the At5g64440 gene product.

Functional Identification of Arabidopsis NAE Amidohydrolase—The *Arabidopsis* putative NAE amidohydrolase was subcloned into pTrcHis and pTrcHis2 for expression in *E. coli* of N-terminal and C-terminal epitope- and polyhistidine-tagged fusion proteins, respectively. *E. coli* lysates were surveyed for expression of enzyme activity using [^{14}C]NAE 18:2 (radiolabeled on the carbonyl carbon) as substrate. Representative chromatograms shown in Fig. 3 indicate that, like the recombinant rat FAAH (expressed in the same vector), the recombinant *Arabidopsis* protein effectively hydrolyzed [1-^{14}C]NAE 18:2 to [1-^{14}C]FFA 18:2. As a control, *E. coli* expressing the *Arabidopsis* cDNA in reverse orientation showed no hydrolytic activity (Fig. 3). In these preliminary experiments with crude *E. coli* lysates, the *Arabidopsis* NAE amidohydrolase activity was linear up to 60 min at protein amounts up to 50 μg. The enzyme was optimally active at alkaline pH (*e.g.* pH 8–9) and was inactivated by treatment at 100 °C for 10 min. The *Arabidopsis* NAE amidohydrolase did not hydrolyze ceramide, nor did ceramide influence NAE hydrolysis (not shown). The *Arabidopsis* NAE amidohydrolase did not catalyze the reverse reaction of NAE hydrolysis (formation of NAE) under any conditions tested (not shown). Higher activity was reproducibly recovered in cells expressing C-terminal fusions, compared with cells expressing N-terminal fusions. Similar to reports for the rat protein (26), the recombinant *Arabidopsis* NAE amidohydrolase was mostly associated with *E. coli* membranes.

Affinity Purification of Recombinant Enzyme—The *Arabidopsis* NAE amidohydrolase, expressed as a C-terminal fusion protein, was solubilized in DDM and subjected to native Ni^{2+}-affinity purification, SDS-PAGE, Western blot analyses, and enzyme activity assays (Fig. 4). A protein of ~70 kDa was enriched under native conditions by Ni^{2+}-affinity purification and was detected by the c-Myc antibody (Fig. 4, *A* and *B*, *arrows*, *Rec. protein lanes*). Likewise, NAE amidohydrolase activity was enriched in this native affinity-purified protein fraction (Fig. 4*C*) by ~375-fold, relative to the DDM-solubilized supernatant (*Supt*) fraction. More stringent denaturing condi-

[2] W. Gish, blast.wustl.edu.

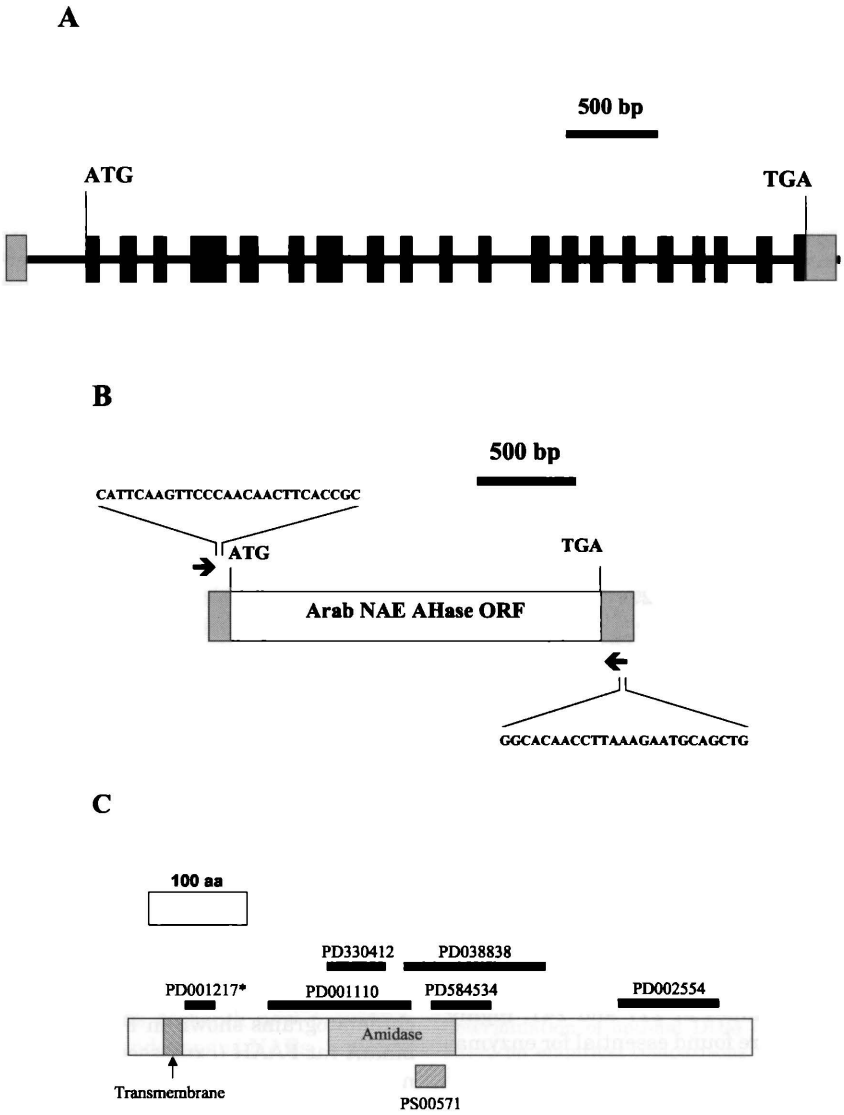

FIG. 1. *A*, the structure and organization of the *Arabidopsis* NAE amidohydrolase genomic sequence (TIGR/TAIR ID At5g64440). This gene is 4689 bp in length, and the predicted protein is 607 amino acids in length with a molecular mass of 66.1 kDa and pI of 6.44. There are 21 exons including 5′-UTR and 3′-UTR (www.tigr.org). The *boxes* represent exons, and *bars* between exons represents introns. The *light shaded boxes* are UTRs. *B*, schematic structure of the cDNA corresponding to *At5g64440*. Sequence-specific RT PCR primers were designed based on the genomic sequence *A. thaliana* (54) annotated at TIGR. The *arrows* denote the position of primers in the 5′- and 3′-UTR. RT-PCR was performed with total RNA extracted from the *Arabidopsis* leaves, and the nucleotide sequence of the isolated cDNA was deposited in GenBank™ (AY308736) and was 99.9% identical to coding region of TC139316 (arabidopsis.org). *C*, schematic of domain organization of predicted *Arabidopsis* NAE amidohydrolase protein. Various domains identified in other proteins with ProDom (20) are depicted *above* the diagram of the polypeptide. These domains are also found in rat FAAH except the one denoted by an *asterisk*. Domains are organized to scale and domain family identifiers (ProDom) are provided. PD038838, from amino acid 271–407, is found in 167 other proteins including a glutamyl-tRNA amidotransferase subunit A from *Methanococcus jannaschii* (Swiss-Prot Q58560). PD001110, from amino acid (*aa*) 138–276, is found in 121 other proteins including a predicted glutamyl-tRNA amidotransferase subunit A from *Aeropyrum pernix* (Swiss-Prot Q9YB80). PD002554, from amino acid 477–575, is found in 173 other proteins including an unknown, predicted amidase from *Homo sapiens* (Swiss-Prot Q9NV19). PD330412, from amino acid 197–253, is found in 64 other proteins including a predicted glutamyl-tRNA amidotransferase subunit A from *Mesorhizobium loti* (Swiss-Prot Q987F8). PD584534, from amino acid 298–358, is found in 36 other proteins including a FAAH from *Rattus norvegicus* (Swiss-Prot P97612). PD001217, from amino acid 60–88, is found in 234 other proteins including a predicted dipeptide binding/transporter protein from *Yersinia pestis* (Swiss-Prot Q8ZA19). PS00571 (PROSITE dictionary) denotes the amidase consensus sequence motif of G(GA)S(GS)(GS)G*X*(GSA)(GSAVY)*X*(LIVM)(GSA)*X*(6)(GSAT) *X*(GA)*X*(DE)*X*(GA)*X*S(LIVM)R*X*P(GSAC) present in all proteins of the amidase class (28, 55–59). A single predicted transmembrane-spanning region *shaded* near the N terminus (TMHMM, Refs. 22 and 23) and the amidase signature sequence (Ref. 31; see Fig. 2*A*) used to conduct the original search for homologues are also diagrammed.

tions led to purification of the recombinant protein to homogeneity (single 70-kDa band on gel), but also inactivated the enzyme irreversibly (not shown). Hence we proceeded with the biochemical characterization of the active enzyme preparation, affinity-purified to near-homogeneity.

Biochemical Characterization—Recombinant NAE amidohydrolase activity was evaluated by incubating affinity-purified NAE amidohydrolase with [1-^{14}C]NAE 20:4, [1-^{14}C]NAE 18:2, [1-^{14}C]NAE 16:0, [1-^{14}C]NAE 14:0, or [1-^{14}C]NAE 12:0 and measuring the rate of conversion to their respective [1-^{14}C]FFA products. NAE amidohydrolase exhibited saturation kinetics with respect to all NAE substrates tested including those identified in plant tissues and those not found in plant tissues. The enzyme exhibited typical Michaelis-Menten kinetics when initial velocity measurements were made at increasing substrate concentrations (Fig. 5), and parameters calculated from these plots are summarized in Table I. The relative apparent K_m values of the *Arabidopsis* enzyme varied by a factor of about 4

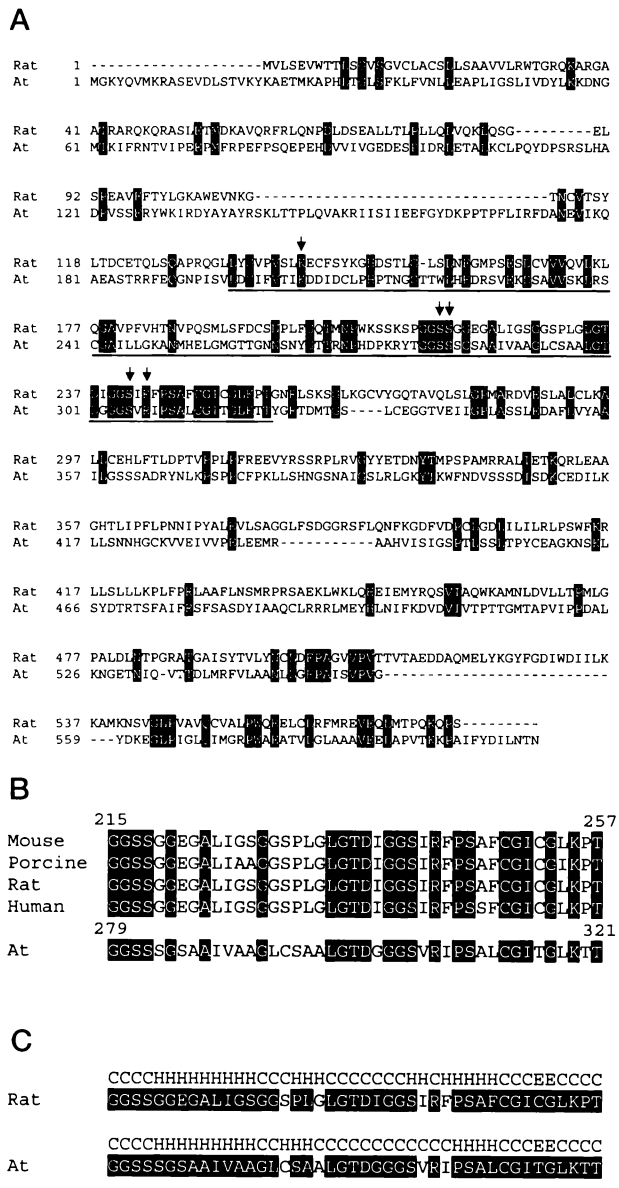

FIG. 2. **Comparative alignment of *Arabidopsis* NAE amidohydrolase amino acid sequence (GenBank™ accession number AY308736) with mammalian FAAH.** *A*, full-length alignment of *Arabidopsis* amino acid sequence (GenBank™ accession number AY308736) with rat FAAH (GenBank™ accession number U72497) (28). These proteins are members of the AS sequence-containing superfamily that includes amidase or amidohydrolase (EC 3.5) enzymes involved in the reduction of organic nitrogen compounds and ammonia production (31, 33). The AS region is *underlined* and consists of about 125 amino acids. There is 18.5% identity between the *Arabidopsis* protein and rat FAAH when compared over the entire length of the proteins, whereas there is 37% identity within the AS. Conserved residues essential for rat FAAH activity (Lys-142, Ser-217, Ser-218, Ser-241, and Arg-243) are indicated with *arrows*. *B*, alignment of more conserved AS sequence motif (30) for the enzymes that hydrolyze NAEs; mouse (GenBank™ accession number U82536) (53), porcine (GenBank™ accession number AB027132) (60), rat (GenBank™ accession number U72497) (28), and human (GenBank™ accession number U82535) (53). Identical residues within this motif between the plant and animal FAAHs are highlighted in *black boxes*. Within this motif there is 55–60% identity between the *Arabidopsis* and mammalian FAAH enzymes. *C*, secondary structure prediction (PSIPRED, 61, 62) of the AS (*C*, coil; *H*, helix; *E*, strand) is depicted *above* the rat and *Arabidopsis* (*At*) AS sequence motifs. Residues with similar secondary structure are highlighted in *black boxes*, illustrating the high degree of similarity within the active site (or AS sequence in NAE amidohydrolase, see Ref. 30). This structural organization has been confirmed for rat FAAH by x-ray crystallography (36) and suggests a functional link between these rat and *Arabidopsis* motif sequences despite limited primary amino acid sequence identity.

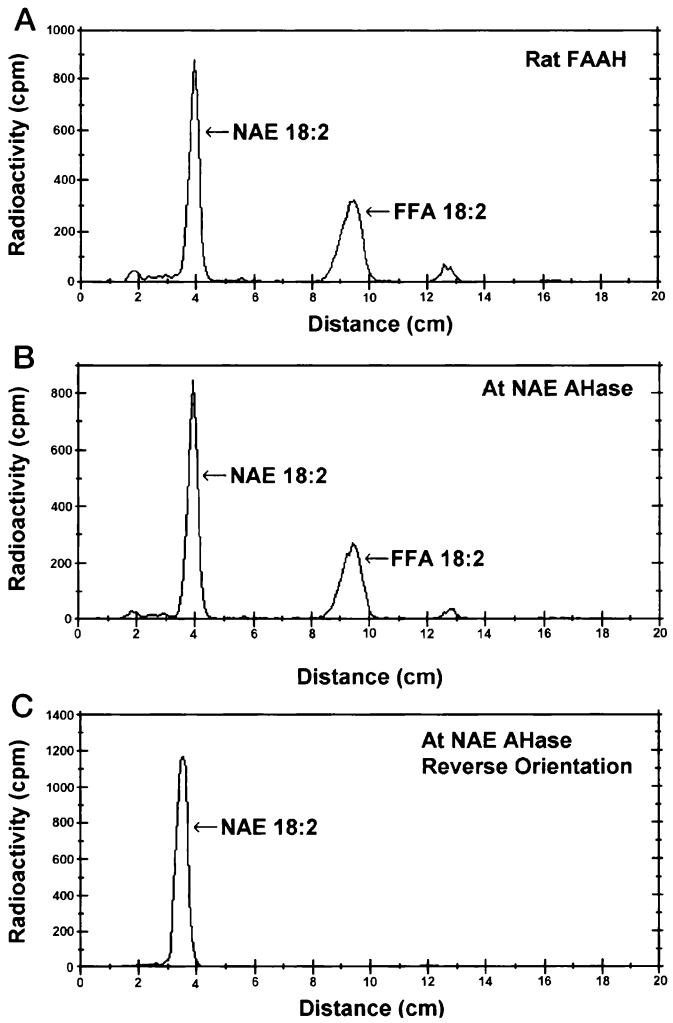

FIG. 3. **Representative radiochromatograms of NAE amidohydrolase activity assays surveyed in *E. coli* harboring expression plasmids.** Lysates from cells expressing recombinant rat FAAH-(*A*) (26) were compared with lysates of cells designed to express the *Arabidopsis* NAE amidohydrolase cDNA in forward (*B*) or reverse orientation (*C*) with respect to the *lacZ* promoter. In all cases cDNAs were in pTrcHis2 expression plasmids, and recombinant protein expression was induced by 4 h of incubation with 1 mM IPTG. For assays, 100 μM [1-^{14}C]NAE 18:2 (~20,000 dpm) in 50 mM BisTris buffer, pH 9.0, was used. The reactions included 50 μg of protein of the respective cell lysate and were incubated for 30 min at 30 °C with shaking. Lipids were extracted and separated by TLC. The positions of [1-^{14}C]NAE 18:2 substrate and [1-^{14}C]FFA product are indicated.

depending upon NAE type. Surprisingly, the *Arabidopsis* enzyme had a higher affinity toward the non-plant NAE 20:4 than toward the more abundant endogenous plant NAE 16:0 and NAE 18:2. The highest maximum rate of NAE hydrolysis also was estimated for NAE 20:4 compared with the endogenous plant NAEs, although the range of the difference was not as great. The specificity constant (k_{cat}/K_m) was calculated for the *Arabidopsis* enzyme toward all NAE substrates and supported the conclusion that NAE 20:4 appeared to be the best substrate for the plant enzyme *in vitro*. Similar published data for the rat FAAH indicated this enzyme showed a 10-fold preference for NAE 20:4 over NAE 16:0 (37). With respect to NAE 20:4, the best substrate for both the plant and animal FAAH, the catalytic efficiency of the *Arabidopsis* NAE amidohydrolase reported here (2.4×10^4 M^{-1} s^{-1}), is about 10 times less than that reported for the rat FAAH (2.2×10^5 M^{-1} s^{-1}). This may be due to different assay conditions, different detergents, or a difference in relative enzyme purity. In any case the same trend was

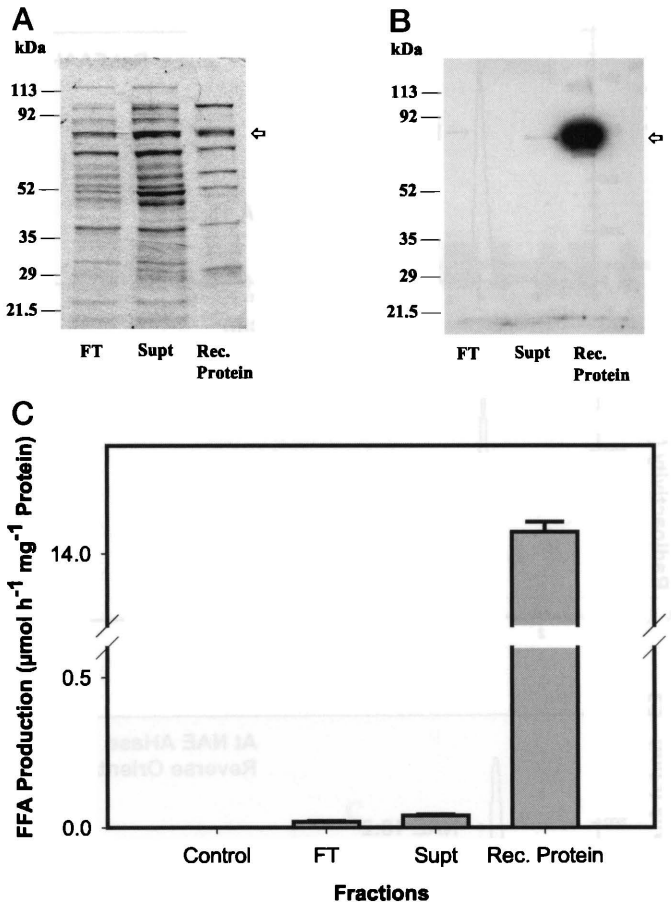

FIG. 4. **SDS-PAGE, Western blot, and activity assays of recombinant *Arabidopsis* NAE amidohydrolase expressed in *E. coli*.** The c-Myc His_6-tagged recombinant protein expressed in *E. coli* was solubilized in DDM and affinity-purified with Ni^{2+} precharged resin (ProBond, Invitrogen) under "native" conditions. *A*, scan of Coomassie Blue (R)-stained SDS gel (10 μg of total proteins in each lane except for *Rec. protein* which was 2 μg) of select fractions. *B*, Western blot analysis of same proteins as in *A*, probed with anti-c-Myc monoclonal antibodies and visualized by indirect chemiluminescence (goat anti-mouse IgG conjugated to horseradish peroxide). The position of the recombinant *Arabidopsis* fusion protein product (predicted to be ~70 kDa) is marked with *open arrows*. Positions of pre-stained standards (not shown) are indicated. *FT* indicates flow-through and represents proteins not specifically bound to the Ni^{2+} resin (pooled 4 washes). *Supt* indicates supernatant and represents total proteins in *E. coli* lysates solubilized in DDM. *Rec. protein* indicates recombinant protein fraction affinity-purified under native conditions. A small but detectable amount of 70-kDa immunoreactive protein was evident in total protein extracts, and as expected this protein was substantially enriched in the affinity purification. *C*, enzymatic assays for NAE 18:2 hydrolysis showed that amidohydrolase activity was enriched coincident with recombinant protein product.

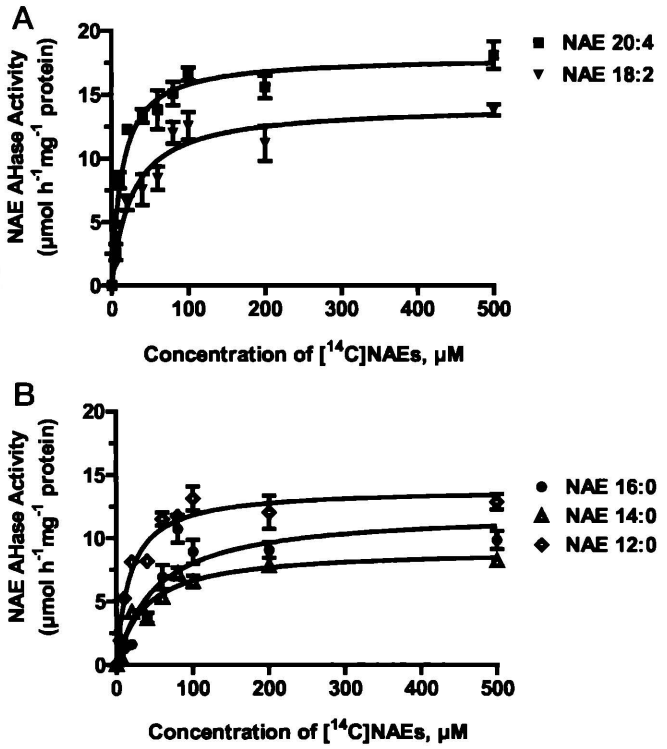

FIG. 5. **Kinetic characterization of affinity-purified recombinant *Arabidopsis* NAE amidohydrolase.** Initial velocity measurements were made at increasing concentrations of respective [1-^{14}C]NAE, combined with appropriate amount of non-radiolabeled NAE to give the final substrate concentration indicated. Reactions were initiated by the addition of 1 μg of recombinant protein and were carried out in 50 mM BisTris buffer, pH 9.0, in a final volume of 800 μl. Reactions were incubated for 30 min with shaking (100 rpm) at 30 °C and stopped by the addition of 2 ml of boiling isopropyl alcohol. Lipids were extracted into chloroform, washed, and separated by TLC (18). Activity was calculated based on the amount of radioactive product formed. Here data points represent means ± S.D. of triplicate assays, all performed on the same "batch" of purified protein. Plots were generated with Prism software version 3.0 (GraphPad Software, San Diego) by fitting the data to the Michaelis-Menten equation. Curve fits yielded correlation coefficients of $r^2 \geq 0.90$ (except for NAE 16:0 where $r^2 = 0.83$), and kinetic parameters summarized in Table I were derived from these plots.

noted for both enzymes in terms of the lower k_{cat}/K_m for NAE 16:0 than for NAE 20:4, despite the much higher levels of endogenous NAE 16:0 content in both systems. These parameters together suggest that the *Arabidopsis* recombinant enzyme recognizes a wide range of NAE types, similar to the situation with mammalian FAAH, and highlights the caution of over-interpreting *in vitro* kinetics data because the best substrate in these studies for the *Arabidopsis* enzyme, NAE 20:4, has not been detected in plants (12).

Two different mechanism-based inhibitors of mammalian FAAH were tested for potency on the hydrolysis of [1-^{14}C]NAE 18:2 by this novel plant NAE amidohydrolase (Table II). PMSF, a nonspecific irreversible serine hydrolase inhibitor that inhibits NAE hydrolysis by mammalian FAAH at low mM concentrations (38), was only modestly effective on the *Arabidopsis* enzyme (inhibited by 44% at 10 mM). However, MAFP, the irreversible active-site targeted inhibitor of rat FAAH (36), completely eliminated NAE hydrolysis by the *Arabidopsis* enzyme at 10 nM. Overall, our biochemical results strongly support the identification of *At5g64440* as a functional homologue of the mammalian FAAH.

DISCUSSION

The results presented here predict and functionally confirm that the *Arabidopsis* gene *AT5g64440* (Fig. 1) encodes a homologue of the mammalian FAAH. Although there was limited primary amino acid sequence identity over the length of the *Arabidopsis* protein compared with the rat protein (18%), there was substantially higher similarity within the amidase catalytic domain both at the primary (37–60% depending on the lengths compared) and secondary structural levels (Fig. 2). Expression of the *Arabidopsis* cDNA in *E. coli* indicated that the *Arabidopsis* protein product was capable of hydrolyzing a wide range of NAE substrates to free fatty acids (Figs. 3–5 and Table I), a feature also of the mammalian enzyme (30, 39). Kinetic parameters summarized in Table I indicated that the plant enzyme has similar affinities for NAE substrates as the FAAH from several mammalian species (28, 39–43). Moreover, the inhibition of the *Arabidopsis* NAE amidohydrolase by

TABLE I

Summary of apparent kinetic parameters of the affinity-purified recombinant A. thaliana NAE amidohydrolase

Parameters were estimated by fitting the data in Fig. 5 to the Michaelis-Menten equation (Prism software, version 3.0, GraphPad).

Substrate	K_m	V_{max}	k_{cat}	k_{cat}/K_m
	M	$\mu mol\ h^{-1}\ mg^{-1}$ protein	s^{-1}	$M^{-1}\ s^{-1}$
NAE 20:4	13.6×10^{-6}	17.9	0.33	2.4×10^4
NAE 18:2	26.2×10^{-6}	14.1	0.26	9.9×10^3
NAE 16:0	50.8×10^{-6}	12.1	0.22	4.3×10^3
NAE 14:0	37.0×10^{-6}	9.1	0.17	4.6×10^3
NAE 12:0	17.6×10^{-6}	13.9	0.26	1.5×10^4

TABLE II

The effects of two mechanism-based inhibitors of mammalian FAAH on the hydrolysis of [-^{14}C]NAE 18:2 by the affinity-purified recombinant Arabidopsis enzyme

Assays were conducted for 30 min at 30 °C in the absence or presence of increasing concentrations of phenylmethylsulfonyl fluoride (PMSF) or methylarachidonyl fluorophosphonate (MAFP). The amount of [1-^{14}C]FFA 18:2 formed was quantified by radiometric scanning following TLC separation of reactions products. The data are means ± S.D. of three replicates and are representative of two experiments.

Concentrations	Specific activity	Relative inhibition
	$\mu mol\ h^{-1}\ mg^{-1}$ protein	%
PMSF		
0 mM	10.56 ± 0.29	0
0.01 mM	11.34 ± 0.55	−7
0.1 mM	9.06 ± 1.86	14
1 mM	7.89 ± 0.37	25
2.5 mM	6.72 ± 0.70	36
10 mM	5.96 ± 0.43	44
MAFP		
0 nM	10.46 ± 0.32	0
0.1 nM	9.69 ± 0.89	7
1 nM	5.62 ± 0.56	46
10 nM	0.00 ± 0.00	100

MAFP (Table II), the active site-directed irreversible inhibitor of rat FAAH (36, 44), strongly suggests a conserved enzyme mechanism between the plant and animal NAE amidases supporting the predictions from sequence/domain comparisons.

We suggest the annotation of "glutamyl-tRNA amidotransferase similarity" now accompanying this *At5g64440* gene be modified to include the new functional information herein regarding NAE hydrolysis. Most amidases, including the mammalian FAAHs, carry the glutamyl-tRNA amidotransferase similarity annotation due to the presence of sequence similarity within the amidase signature domain, often as the only identifiable domain within this family of proteins. Based on our functional studies, it is unlikely that this At5g64440 gene product functions as a glutamyl-tRNA amidotransferase, and this activity has not been attributed to membrane-bound mammalian FAAH enzymes. Additionally, in plants these glutamyl-tRNA amidotransferases are localized in the stroma of chloroplasts as soluble, oligomeric complexes of multiple subunits (45, 46). In fact, nuclear-encoded, chloroplast-localized orthologues of the glutamyl-tRNA amidotransferase subunits have been cloned from *Arabidopsis* and expressed/characterized by the Soll group (GenBank™ accession numbers, AF241841, AF240465, AF239836, and AF224745), and these proteins share less than 24% amino acid sequence identity with the At5g64440 NAE amidohydrolase. Thus there is a need to clarify the descriptive annotation within these amidase protein subfamilies.

The signal-mediated activation of NAE metabolism constitutes a major regulatory feature of the endocannabinoid signaling system in animal tissues through the rapid generation and timely degradation of bioactive acylethanolamides (4, 9, 28, 47, 48). Although a principal role for NAE 20:4 as an endogenous ligand for cannabinoid receptors has emerged as a paradigm for endocannabinoid signaling (2, 38), other types of NAEs as well as other fatty acid derivatives likely interact with this pathway directly or indirectly to modulate a variety of physiological functions in vertebrates (49–52). An increasingly detailed understanding of the degradation of these bioactive NAEs by FAAH has pointed to this metabolic step as a key regulator of NAE levels and hence NAE function *in vivo* (9, 29, 30). Recent major advances in the understanding of FAAH function in mammals at the structural level (36), mechanistic level (32), and the physiological level (9) have been made possible only through the cloning, expression, and manipulation of the cDNA/gene encoding FAAH (53). We anticipate the identification of this plant cDNA will facilitate a similar increased appreciation for this lipid pathway in plant physiology.

Research in the last decade has made it apparent that NAE metabolism occurs in plants by pathways analogous to those in vertebrates and invertebrates (12, 18), pointing to the possibility that these lipids may be part of an evolutionarily conserved mechanism for the regulation of physiology in multicellular organisms. Two physiological situations in plant systems have been identified in which the endogenous levels of NAEs are transiently modulated. The first is in the perception of fungal elicitors by plant cells, wherein the levels of endogenous NAE 14:0 were elevated 10–50-fold in leaves of tobacco plants following elicitation (17). In other work, NAEs (mostly C12, C16, and C18 types) were quantified in desiccated seeds of higher plants but were metabolized rapidly during the first few hours of seed imbibition/germination (10), in part by an amidohydrolase-mediated pathway (18), suggesting that the transient changes in NAE content may play a role in seed germination. In fact, *Arabidopsis* seedlings germinated and grown in the presence of exogenous NAE exhibited dramatically altered developmental organization of root tissues (15).

With evidence of conserved enzymatic machinery in plants for the formation and degradation of NAEs, and the potent biological effects caused by altered exogenous NAE levels, it is now important to begin to address NAE function in plants by forward and reverse genetics approaches. The identification of an *Arabidopsis* cDNA clone encoding a functional NAE amidohydrolase re-enforces the similarity between plants and animals in terms of NAE metabolism, but more importantly provides a tool for the future manipulation of NAE levels in plants as a means to understand the physiological role(s) of these bioactive lipids in the plant kingdom.

Acknowledgments—We thank Drs. John Ohlrogge and Fred Beisson, Michigan State University, for sharing their catalogue of *Arabidopsis* lipid genes in advance of its publication. Dr. Cecilia Hillard, Medical College of Wisconsin, with permission of Dr. Benjamin Cravatt, Scripps Research Institute, kindly provided the cloned rat WT-FAAH and Δ TM-FAAH in pTrcHis2 for our studies.

REFERENCES

1. Schmid, H. H. O., Schmid, P. C., and Nataranjan, V. (1996) *Chem. Phys. Lipids* **80,** 133–142
2. Wilson, R. I., and Nicoll, R. A. (2002) *Science* **296,** 678–682
3. Pertwee, R. G. (2001) *Prog. Neurobiol.* **63,** 569–611
4. Hansen, H. S., Moesgaard, B., Hansen, H. H., and Petersen, G. (2000) *Chem. Phys. Lipids.* **108,** 135–150

5. Van der Stelt, M., Veldhuis, W. B., Van Haaften, G. W., Fezza, F., Bisogno, T., Bar, P. R., Veldink, G. A., Vliegenthart, J. F. G., Di Marzo, V., and Nicolay, K. (2001) *J. Neurosci.* **21,** 8765–8771
6. Buckley, N. E., McCoy, K. L., Mezey, E., Bonner, T., Zimmer, A., Felder, C. C., Glass, M., and Zimmer, A. (2000) *Eur. J. Pharmacol.* **396,** 141–149
7. Paria, B. C., and Dey, S. K. (2000) *Chem. Phys. Lipids* **108,** 211–220
8. Sarker, K. P., Obara, S., Nakata, M., Kitajima, I., and Maruyama, I. (2000) *FEBS Lett.* **472,** 39–44
9. Cravatt, B. F., and Lichtman, A. H. (2002) *Chem. Phys. Lipids* **121,** 135–148
10. Chapman, K. D., Venables, B. J., Markovic, R., Blair, R. W., and Bettinger, C. (1999) *Plant Physiol.* **120,** 1157–1164
11. Schmid, H. H. O., Schmid, P. C., and Nataranjan, V. (1990) *Prog. Lipid Res.* **29,** 1–43
12. Chapman, K. D. (2000) *Chem. Phys. Lipids* **108,** 221–230
13. Chapman, K. D., Tripathy, S., Venables, B. J., and Desouza, A. D. (1998) *Plant Physiol.* **116,** 1163–1168
14. Pappan, K., Austin-Brown, S., Chapman, K. D., and Wang, X. (1998) *Arch. Biochem. Biophys.* **353,** 131–140
15. Blancaflor, E. B., Hou, G., and Chapman, K. D. (2003) *Planta* **217,** 206–217
16. Tripathy, S., Kleppinger-Sparace, K., Dixon, R. A., and Chapman, K. D. (2003) *Plant Physiol.* **131,** 1781–1791
17. Tripathy, S., Venables, B. J., and Chapman, K. D. (1999) *Plant Physiol.* **121,** 1299–1308
18. Shrestha, R., Noordermeer, M. A., Vand der Stelt, M., Veldenk, G. A., and Chapman, K. D. (2002) *Plant Physiol.* **130,** 391–401
19. Hillard, C. J., Edgemond, W. S., and Campbell, W. B. (1995) *J. Neurochem.* **64,** 677–683
20. Servant, F., Bru, C., Carrère, S., Courcelle, E., Gouzy, J., Peyruc, D., and Kahn, D. (2002) *Brief. Bioinform.* **3,** 246–251
21. Sigrist C. J., Cerutti L., Hulo N., Gattiker A., Falquet L., Pagni M., Bairoch A., and Bucher, P. (2002) *Brief. Bioinform.* **3,** 265–274
22. Krogh, A., Larsson, B., von Heijne, G., and Sonnhammer, E. L. (2001) *J. Mol. Biol.* **305,** 567–580
23. Sonnhammer, E. L., von Heijne, G., and Krogh, A. (1998) *Proc. Int. Conf. Intell. Syst. Mol. Biol.* **6,** 175–182
24. Nakai, K., and Kanehisa, M. (1992) *Genomics* **14,** 897–911
25. Elbing, K., and Brent, R. (2002) in *Current Protocols in Molecular Biology* (Ausubel, F. M., Brent, R., Kingston, R. E., Moore, D. D., Seidman, J. G., Smith, J. A., and Struhl, K., eds) Vol. 1, pp. 1.2.1–1.2.2, John Wiley and Sons, New York
26. Patricelli, M. P., Lashuel, H. A., Giang, D. K., Kelly, J. W., and Cravatt, B. F. (1998) *Biochemistry* **37,** 15177–15187
27. Bradford, M. M. (1976) *Anal. Biochem.* **72,** 248–254
28. Cravatt, B. F., Giang, D. K., Mayfield, S. P., Boger, D. L., Lerner, R. A., and Gilula, N. B. (1996) *Nature* **384,** 83–87
29. Ueda, N. (2002) *Prostaglandins & Other Lipid Mediators* **68,** 521–534
30. Ueda, N., Puffernbarger, R. A., Yamamoto, S., and Deutsch, D. G. (2000) *Chem. Phys. Lipids* **108,** 107–121
31. Patricelli, M. P., and Cravatt, B. F. (2000) *J. Biol. Chem.* **275,** 19177–19184
32. McKinney, M. K., and Cravatt, B. F. (May 6, 2003) *J. Biol. Chem.* 10.1074/jbc.M303922200
33. Chebrou, H., Bigey, F., Arnaud, A., and Galzy, P. (1996) *Biochim. Biophys. Acta* **1298,** 185–293
34. Omeir, R. L., Arreaza, G., and Deutsch, D. G. (1999) *Biochem. Biophys. Res. Commun.* **264,** 316–320
35. Patricelli, M. P., Lovato, M. A., and Cravatt, B. F. (1999) *Biochemistry* **38,** 9804–9812
36. Bracey, M. H., Hanson, M. A., Masuda, K. R., Stevens, R. C., and Cravatt, B. F. (2002) *Science* **298,** 1793–1796
37. Katayama, K., Ueda, N., Katoh, I., and Yamamoto, S. (1999) *Biochim. Biophys. Acta* **1440,** 205–214
38. Desarnaud, F., Cadas, H., and Piomelli, D. (1995) *J. Biol. Chem.* **270,** 6030–6035
39. Boger, D. L., Fecik, R. A., Patterson, J. E., Miyauchi, H., Patricelli, M. P., and Cravatt, B. F. (2000) *Bioorg. Med. Chem. Lett.* **10,** 2613–2616
40. Fowler, C. J., Jonsson, K.-O., and Tiger, G. (2001) *Biochem. Pharmacol.* **62,** 517–526
41. Pertwee, R. G., Fernando, S. R., Griffin, G., Abadji, V., and Makriyannis, A. (1995) *Eur. J. Pharmacol.* **272,** 73–78
42. Bisogno, T., Maurelli, S., and Tiger, G. (1997) *J. Biol. Chem.* **272,** 3315–3323
43. Tiger, G., Stentrom, A., and Fowler, C. J. (2000) *Biochem. Pharmacol.* **59,** 647–653
44. Deutsch, D. G., Omeir, R., Arreaza, G., Salehani, D., Prestwich, G. D., Huang, Z., and Howlett, A. (1997) *Biochem. Pharmacol.* **53,** 255–260
45. Schon, A., Kannangara, C. G., Gough, S., and Soll, D. (1988) *Nature* **331,** 187–190
46. Becker, H. D., Min, B., Jocobi, C., Reczniak, G., Pelaschier, J., Roy, H., Klein, S., Kern, D., and Soll, D. (2000) *FEBS Lett.* **476,** 140–144
47. Hillard, C. J. (2000) *Prostaglandins & Other Lipid Mediators* **61,** 3–18
48. Bisogno, T., De Petrocellis, L., and Di Marzo, V. (2002) *Curr. Pharm. Design* **8,** 125–133
49. Lambert, D. M., and Di Marzo, V. (1999) *Curr. Med. Chem.* **6,** 663–674
50. Lambert, D. M., Vandevoorde, K. O., and Fowler, C. F. (2002) *Curr. Med. Chem.* **9,** 739–755
51. Schmid, H. H., and Berdyshev, E. V. (2002) *Prostaglandins Leukot. Essent. Fatty Acids* **66,** 363–376
52. Schmid, H. H. O., Schmid, P. O., and Berdyshev, E. V. (2002) *Chem. Phys. Lipids* **121,** 111–134
53. Giang, D. K., and Cravatt, B. F. (1997) *Proc. Natl. Acad. Sci. U. S. A.* **94,** 2238–2242
54. Arabidopsis Genomic Initiative (2000) *Nature* **408,** 796–815
55. Mayaux, J. F., Cerbelaud, E., Soubrier, F., Faucher, D., and Petre, D. (1990) *J. Bacteriol.* **172,** 6764–6773
56. Hashimoto, Y., Nishiyama, M., Ikehata, O., Horinauchi, S., and Beppu, T. (1991) *Biochim. Biophys. Acta* **1088,** 225–233
57. Chang, T. H., and Abelson, J. (1990) *Nucleic Acids Res.* **18,** 7180–7180
58. Tsuchiya, K., Fukuyama, S., Kanzaki, N., Kanagawa, K., Negoro, S., and Okada, H. (1989) *J. Bacteriol.* **171,** 3187–3191
59. Curnow, A. W., Hong, K. W., Yuan, R., Kim, S. I., Martins, O., Winkler, W., Henkin, T. M., and Soll, D. (1997) *Proc. Natl. Acad. Sci. U. S. A.* **94,** 11819–11826
60. Goparaju, S. K., Kurahashi, Y., Suzuki, H., Ueda, N., and Yamamoto, S. (1999) *Biochim. Biophys. Acta* **1441,** 77–84
61. McGuffin, L. J., Bryson, K., and Jones, D. T. (2000) *Bioinformatics* **16,** 404–405
62. Jones, D. T. (1999) *J. Mol. Biol.* **292,** 195–202